8B.6 MODELING AND EXPERIMENTAL OBSERVATIONS OF WEATHER RADAR GROUND CLUTTER

J.C. Hubbert*, G. Meymaris, M. Dixon, and S. Ellis
National Center for Atmospheric Research, Boulder CO

1 INTRODUCTION

The mitigation of ground clutter for weather radars is an important aspect of data quality and interpretation of echoes. Recently a ground clutter identification technique was introduced that robustly detects ground clutter contaminated signals in real time (Hubbert et al. 2009b,a) named Clutter Mitigation Decision (CMD). In Hubbert et al. (2009b) a clutter metric CPA (Clutter Phase Alignment) is introduced that is shown to be an effective clutter discriminator. It is based on the idea that echoes from stationary ground clutter targets are constant (assuming that the radar scan angle changes very little). This means that phase of the complex in-phase (I) and quadrature components (Q), $\arg\{I + jQ\}$, is constant so that

$$CPA = \left| \sum_{i=1}^{N} x_i \right| / \left[\sum_{i=1}^{N} |x_i| \right] \approx 1. \quad (1)$$

where x_i is the complex times series corresponding to a radar resolution volume. Thus, typical ground clutter targets have $CPA > 0.9$ while for weather targets, $CPA < 0.6$. Recently collected experimental radar data revealed a few ground clutter target which possessed very low CPA. A distinguishing feature is that the spectrum of these data show a double peak close to zero velocity. This paper explains the nature of such ground clutter targets.

This paper also investigates the spectrum width of ground clutter signals using both modeled data and experimental data from S-Pol, NCAR's S-band polarimetric radar. A new estimator for narrow spectrum widths is introduced.

2 "DOUBLE PEAKED" CLUTTER SPECTRA

Experimental radar data from the NEXRAD KEMX in Flagstaff, Arizona show anomalous ground clutter targets with very low, uncharacteristic CPA values. The low CPA values cause the CMD algorithm to misclassify these pixels as weather instead of clutter. Though rare, it is of interest to explain the cause and nature of such anomalous echoes. Shown in Fig. 1 is an example of such data. The top panel (a) shows the power spectrum and the double peak close to zero velocity (center vertical line in the panel). Since the numerator of CPA (Eq.(1)) is the vector sum of the time series values, the low value of CPA can be explained by examining the magnitude and phase of the time series shown in panels (b) and (c), respectively. Note the high, close to equal power at the beginning and end of the time series; then note that the phase at the beginning and end of the time series is about 180° degrees apart. Thus the vector sum of the complex numbers will be relatively small. Alternately, it is seen in the power spectrum that there is a reduction of power at zero velocity relative to the surrounding spectral points. Examining the real and imaginary parts of panels (d) and (e), respectively, it is seem that the curves cross zero and have both negative and positive values. Since the zero velocity component is proportional to $(\sum i)^2 + (\sum q)^2$, the sum of these negative and positive values have a tendency to reduce the zero velocity component relative to the surround velocity components.

To explain the the physical nature of clutter targets that can cause such signatures, we use the clutter model presented in Hubbert et al. (2009b). Shown in Fig. 2 is a schematic of the clutter model for 64 point sampling. There are 256 scattering centers and the radar beam is modeled as Gaussian with 192 points. The 3 dB beam width is 64 points. Radar time series samples are generated by convolving the radar beam with the scattering centers. One scattering center is considered dominant, larger in magnitude than the other scattering centers and is constant.The other scattering centers are modeled as Rayleigh random variables. Form more details see Hubbert et al. (2009b).

This model model, however, does not produce times series with double peaks in the spectrum as discussed above. This can be explained if there are two dominant scatterers in the radar resolution volume. These two dominant scatterers must be characterized with phase shifts upon backscatter that are about 180° apart and scattering magnitudes that are similar. Shown in Fig. 3 is the power spectrum of simulated data resulting from the model. As can be seen, there is a deep minimum at zero velocity. Shown in Figs. 4 and 5 are the real and imaginary parts, and the magnitude and phase, respectively. As explained above, these plots demonstrate why there is minimum at

*NCAR/EOL, Boulder, Colorado 80307, email: hubbert@ucar.edu

zero velocity, at least mathematically. Such signatures are are fairly rare. The CPA of such clutter targets are typically less that 0.2 so that CMD will consistently classify such echoes are weather. To mitigate this, the calculation of CPA can be broken into two parts defined by the location of the minimum of the time series magnitude.

3 ESTIMATING THE SPECTRUM WIDTH

The typical estimators of spectrum for ground clutter echoes have variance if only a few samples are available, i.e. less than about 100 samples (Doviak and Zrnić 1993). The difficulty was illustrated in Hubbert et al. (2009b). For narrow spectrum width signals, frequently $|R_1| > R_0$ where R_0 and R_1 are the zeroth and first lag of the autocorrelation function (the zeroth lag is power). This causes the so called R_0, R_1 spectrum width estimator to be undefined. Many authors set the spectrum width to zero when $|R_1| > R_0$. As shown in Hubbert et al. (2009b), when modeling weather signals with 64 samples for spectrum width of 0.5 m/s, at S-band with a $PRT = 0.001$ s, about 42% of the generated time series will have $|R_1| > R_0$, and the histogram is given here in Fig. 6 (Hubbert et al. 2009b). The mean spectrum width estimate of the remaining 58% of the time series is 1.1 m/s. Clearly, the R_0, R_1 spectrum width estimator does not yield an accurate estimate of the spectrum width of narrow spectrum with signals. Thus, if the spectrum width narrow spectrum width of clutter is to be investigated experimentally, a better spectrum width estimator needs to be found.

Better spectrum width estimation (improved bias and variance) can be accomplished by fitting a Gaussian curve to the first 6 lags of the autocorrelation function. This is done by first taking the logarithm of the autocorrelation function and then performing a quadratic fit. Shown in Fig. 7 are 10 sample autocorrelation functions (magnitude) for a spectrum width of 0.2 m/s, $PRT = 0.001$ s, S-band, 64 samples. A rectangular window is used on the time series. A quadratic fit to the first 7 lags (0 through 6) of the autocorrelation function is used to estimate the spectrum width. For this simulation, 38% of the generated time series yielded a spectrum width of zero. To understand this, view the top two autocorrelation curves in Fig. 7. The curves are normalized so that the zeroth lag (power) of each time series is 1. As can be seen, the top two curves actually become greater than 1which is physically meaningless. Figure 8 show one such auto correlation plot. Note that the autocorrelation values are greater than one out beyond 20 lags! When this occurs, the spectrum width estimate is set to zero. This phenomena is due to the finite length of the time series and the unbiased autocorrelation estimate (Hubbert et al. 2009b; Bringi and Chandrasekar 2001). The accuracy of the spectrum width estimate can be improved if a Hamming window is used on the time series and then the autocorrelation function is calculated. The number of zero width estimates is then reduced from 38% to 13%. Figure 9 shows the mean (bias) and standard deviation versus spectrum width for simulated data when a Hamming window is used. The resulting autocorrelation function is compensated taking into account the autocorrelation function of the window function by itself (the auto correlation function of the data is affected (biased) by the used window function). Figure 10 shows a histogram of the simulated data for a spectrum width of 0.2 m/s while Fig. 11 shows a histogram for a spectrum width of 0.5 m/s. Compare Fig. 11 to the previous Fig. 6 which uses the R_0/R_1 estimator. The 7-lag estimator shows much less variance and has a bias of only -0.1m/s.

This 7-lag spectrum width estimator is now used for experimental data. The objective is to experimentally investigate the spectrum with of ground clutter for various scan rates and dwell angles. We first vary the scan rate of S-Pol while maintaining the same dwell angle of of 1°. The scan rates are 2.5°s^{-1}, 5.0°s^{-1}, 7.5°s^{-1}, 10.0°s^{-1} and 12.5°s^{-1}. Shown in Figs. 12 and 13 are histograms for the scan rates of 2.5°s^{-1} and 12.5°s^{-1}, respectively. The means are 0.05 m s^{-1} and 0.24 m s^{-1}. The increase in the mean value and the increase in variance can be attributed to the increase in scan rate. Figure 14 shows the mean estimated spectrum widths versus scan rate with the blue curve. The red curve is a straight line fit with the slope and intercept given on the plot.

4 SUMMARY AND CONCLUSIONS

This paper has examined 1) an anomalous double-peaked ground clutter spectrum, 2) a new spectrum width estimator for narrow spectrum widths and 3) applied the new spectrum width estimator to experimental S-Pol data.

The anomalous double-peaked spectra were explained and modeled by having two dominant clutter targets such that their phase shift upon backscatter differed by 180°. These such clutter targets, while rare, are important to identify since they cause the clutter metric CPA (Clutter Phase Alignment) to be very low and in turn cause CMD (Clutter Mitigation Decision), to incorrectly misclassify the echo as weather. The CPA calculation has been modified to correctly identify such echoes as clutter.

A new spectrum width estimator was given that fits a Gaussian curve to the first 7-lags of the auto correlation function. The performance of this estimator has greatly reduce bias and variance as compared to the traditional R_0/R_1 estimator for narrow spectrum widths.

The new 7-lag estimator was then applied to experimental S-Pol data to investigate the effects of radar scan rate on spectrum width estimates.

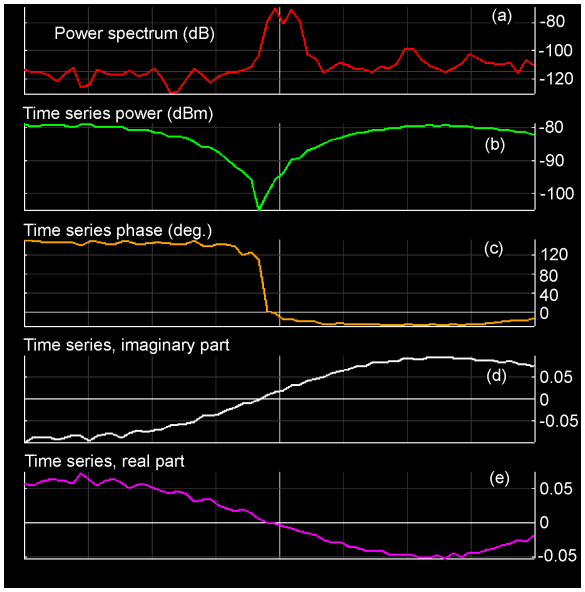

Figure 1: *An example "double peaked" anomalous ground clutter return (time series). CPA is about 0.1 which is indicative weather echoes.*

Acknowledgment This research was supported in part by the ROC (Radar Operations Center) of Norman OK. The National Center for Atmospheric Research is sponsored by the National Science Foundation. Any opinions, findings and conclusions or recommendations expressed in this publication are those of the author(s) and do not necessarily reflect the views of the National Science Foundation.

References

Bringi, V. and V. Chandrasekar, 2001: *Polarimetric Doppler Weather Radar*. Cambridge Univ. Press, Cambridge, UK.

Doviak, R. and D. Zrnić, 1993: *Doppler Radar and Weather Observations*. Academic Press, 2^{nd} edition.

Hubbert, J., M. Dixon, and S. Ellis, 2009a: Weather radar ground clutter, Part II: real-time identification and filtering. *J. Atmos. Oceanic Technol.*, **26**, 1181–1197.

Hubbert, J., M. Dixon, S. Ellis, and G. Meymaris, 2009b: Weather radar ground clutter, Part I: identification, modeling and simulation. *J. Atmos. Oceanic Technol.*, **26**, 1165–1180.

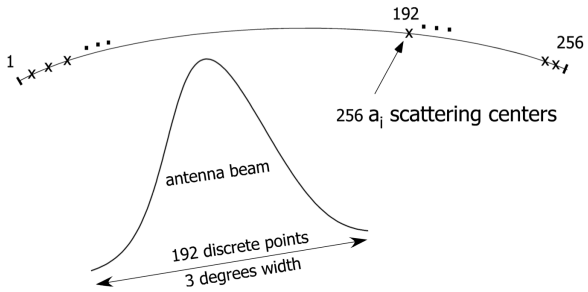

Figure 2: *Clutter model.*

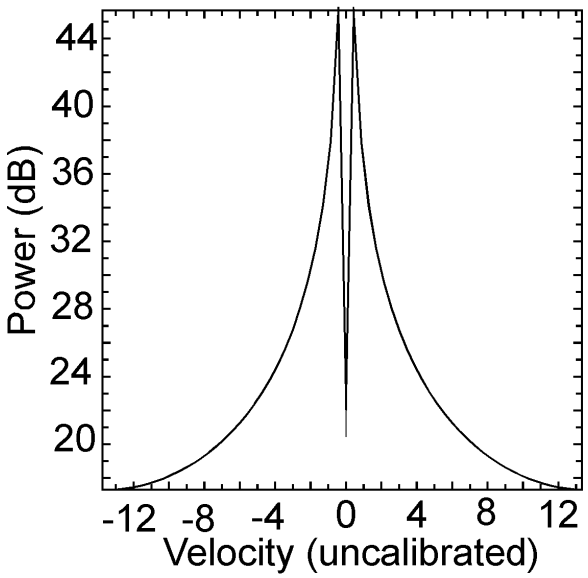

Figure 3: *Power spectrum of modeled data showing a doubled peaked spectrum..*

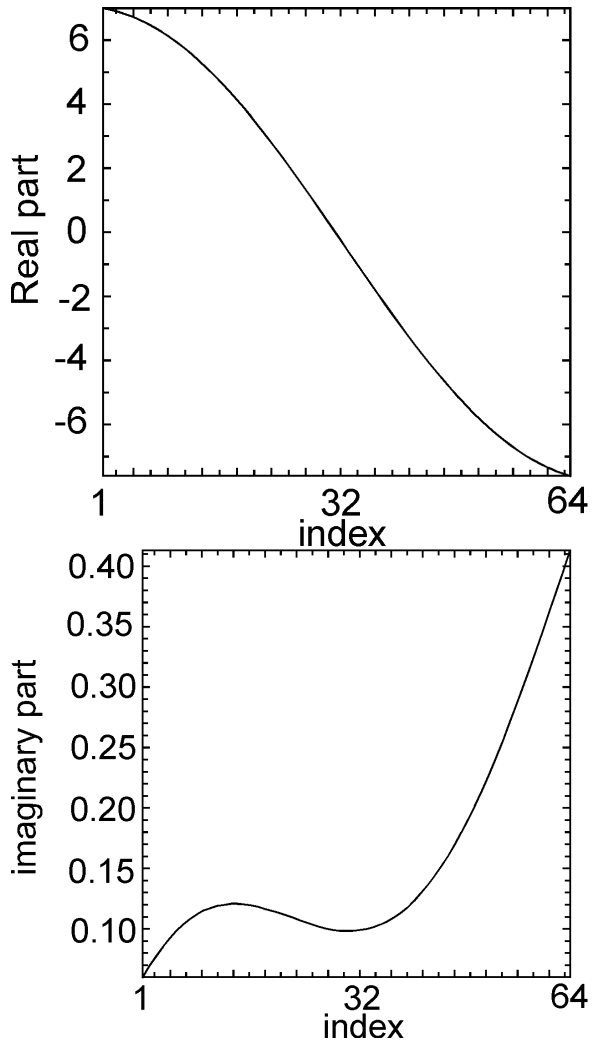

Figure 4: *Top: real part of time series; Bottom: imaginary part of time series, corresponding to Fig. 3.*

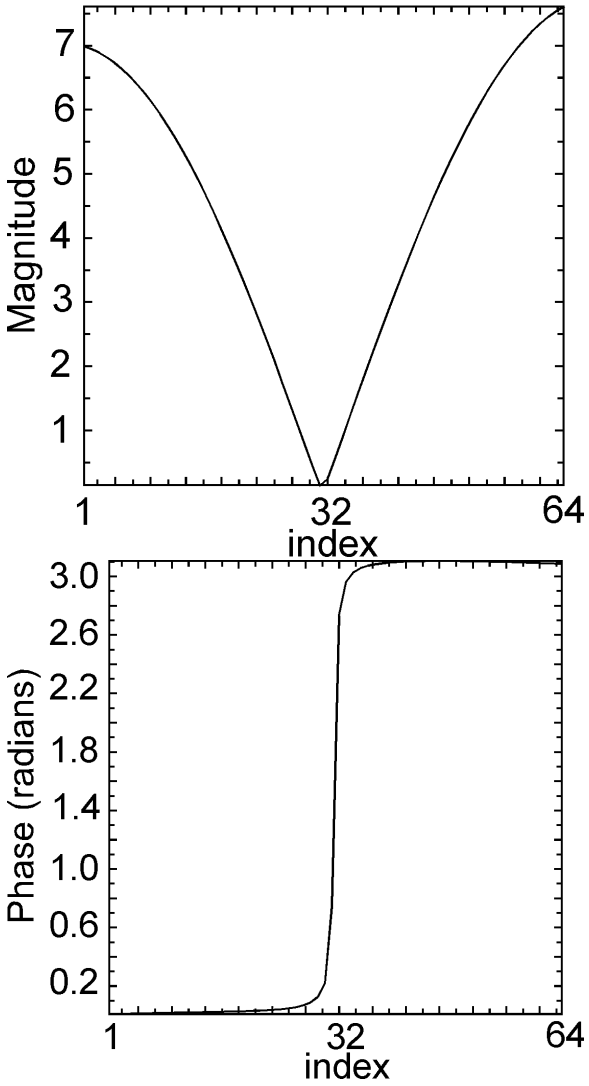

Figure 5: *Top: magnitude of time series; Bottom: phase of time series corresponding to Fig. 3.*

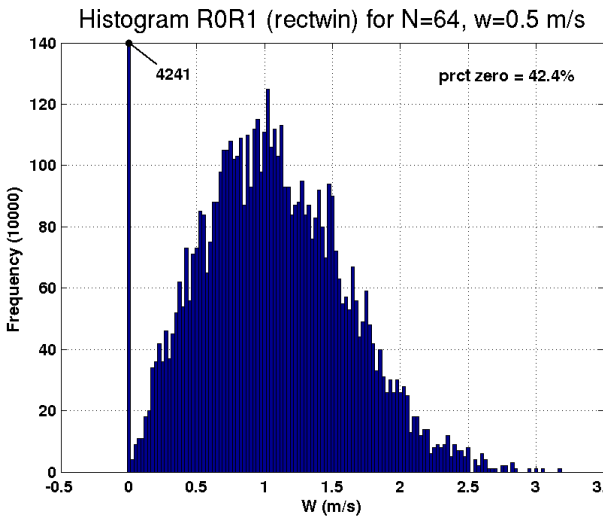

Figure 6: *Spectrum width histogram for simulated data. Simulation parameters: spectrum width = 0.5 m/s, PRT =0.001 s, S-band, 64 points SNR= 100 dB. 42.4% of the estimates have* $|R_1| > R_0$ *that are assigned a value of zero m/s.*

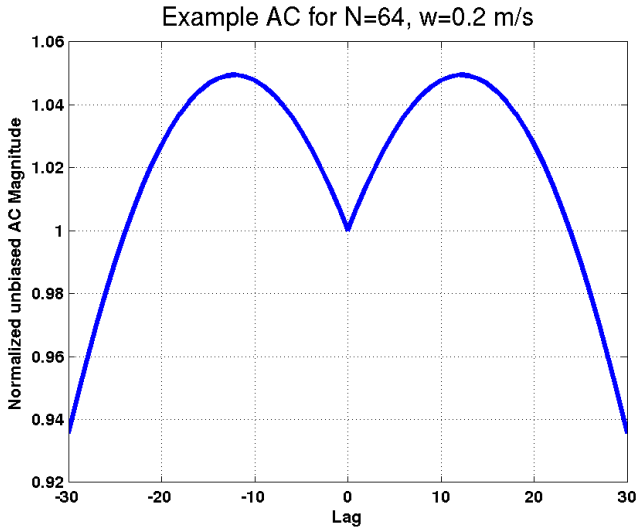

Figure 8: *Auto correlation plot for simulated data. Simulation parameters: spectrum width = 0.2 m/s, PRT =0.001 s, S-band, 64 points SNR= 100 dB.*

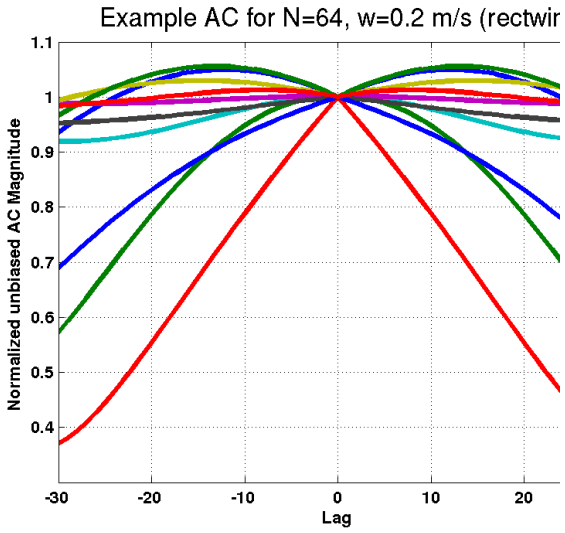

Figure 7: *Auto correlation plots for simulated data. Simulation parameters: spectrum width = 0.2 m/s, PRT =0.001 s, S-band, 64 points SNR= 100 dB.*

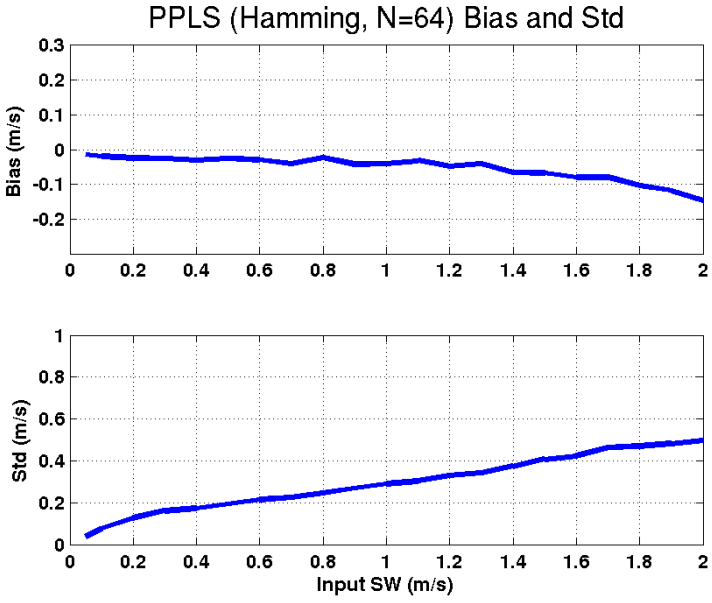

Figure 9: *The mean and standard deviation of simulated data as a function of spectrum width. Simulation parameters: PRT =0.001 s, S-band, 64 points, SNR= 100 dB. The 7-lag estimator is use.*

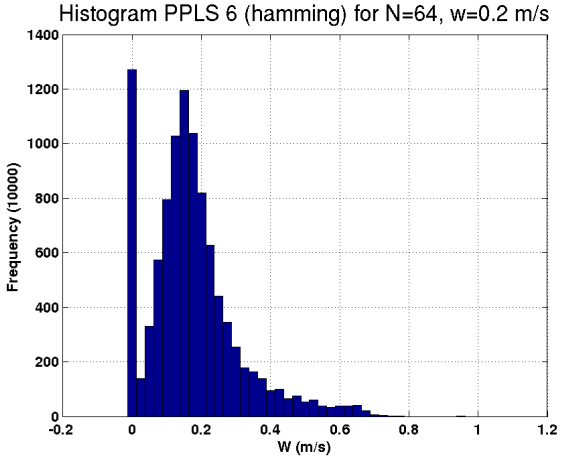

Figure 10: *Histogram of spectrum width estimates for simulated data. Simulation parameters: spectrum width = 0.2 m/s, PRT =0.001 s, S-band, 64 points SNR= 100 dB.*

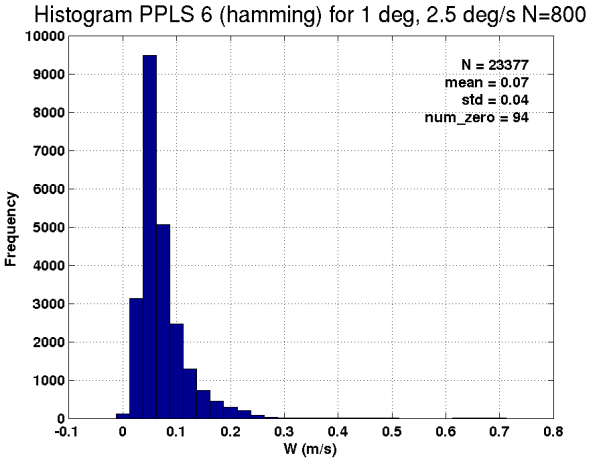

Figure 12: *Histogram of spectrum width estimates for experimental data gathered by S-pol. The dwell angle is 1° and the scan rate is 2.5°s^{-1}.*

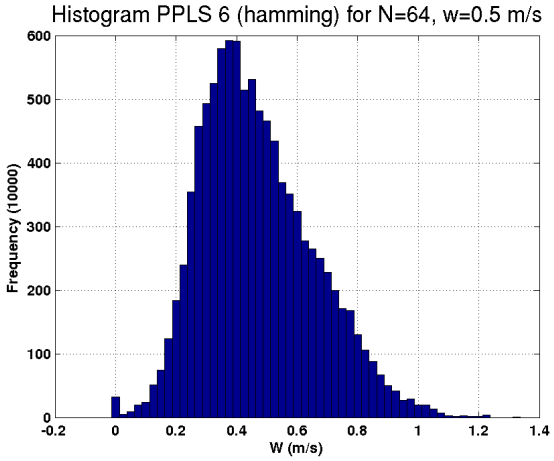

Figure 11: *Histogram of spectrum width estimates for simulated data. Simulation parameters: spectrum width = 0.5 m/s, PRT =0.001 s, S-band, 64 points SNR= 100 dB*

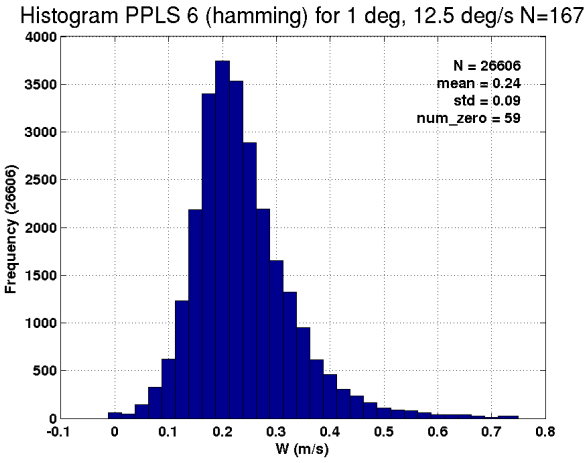

Figure 13: *Histogram of spectrum width estimates for experimental data gathered by S-pol. The dwell angle is 1° and the scan rate is 12.5°s^{-1}.*

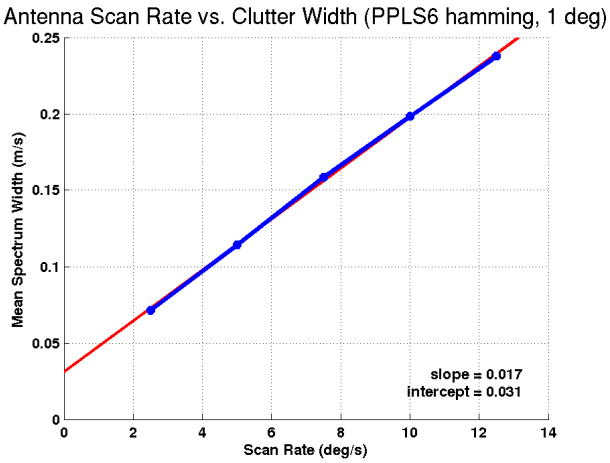

Figure 14: *Spectrum width versus radar scan rate for experimental S-Pol clutter data. The dwell angle is1°. The red curve is a least squares straight line fit.*